Proc. Natl. Sci. Counc. ROC(A)
Vol. 19, No. 4, 1995. pp. 334-341

A Multivariable Sliding Mode Control for Magnetic Suspension Systems

LAIN-SHIN HUNG AND SHIH-CHANG LIN

Department of Power Mechanical Engineering
National Tsing-Hua University
Hsin-Chu, Taiwan, R.O.C.

(Received November 14, 1994; Accepted December 9, 1994)

ABSTRACT

This paper presents a practical design and implementation method of multivariable sliding mode control for magnetic suspension systems in the presence of parameter variations and external disturbances. Based on the Lyapunov function approach, the proposed design method ensures the existence of a control law to satisfy the sliding mode condition. The designed controller was successfully implemented in an experimental magnetic suspension system. Experimental results showed that the system was well under the control of predeterminate sliding mode dynamics and verified the capabilities of the controller. Furthermore, this paper provides a real case of experimental study on multivariable sliding mode control.

Key Words: multivariable sliding model control, magnetic suspension

I. Introduction

This paper presents a design and implementation method of multivariable sliding mode control for magnetic suspension systems in the presence of parameter variations and external disturbances. Magnetic suspension systems have been successfully demonstrated for many applications, including magnetic bearings, high-speed trains and material handling devices (Jayawant, 1988; Matsumura, 1993). Because of the inherent instability of magnetic suspension systems, an active control is usually required to stabilize systems which in nature are multi-dimensional dynamic systems. The number of axes that require active control depends on the system structure. For example, there are so-called two-axis, three-axis, and five-axis active control magnetic suspension systems (Matsumura, 1993). For multi-axis active control magnetic suspension systems, ideally, multivariable control should be used; in reality, using the scheme of single-input single-output control for each axis has been a common practice in the literature.

In recent years, two well-known robust control methods, H^∞ control (Matsumura *et al.*, 1991; Cui and Nonami, 1992) and sliding mode control (Misovec *et al.*, 1990; Hwang, 1992; Hwang *et al.*, 1992; Nonami and Yamaguchi, 1992; Cho *et al.*, 1993) have been successfully applied to magnetic suspension systems. Compared with H^∞ control, sliding mode control is easier to design and implement. In addition, sliding mode control can be easily extended to handle the dynamic nonlinearity inherent in magnetic suspension systems (Misovec *et al.*, 1990; Hwang, 1992) while H^∞ control is strictly based on the linear control structure. Therefore, sliding mode control for magnetic suspension systems deserves further study. First of all, multivariable sliding mode control should be employed for magnetic suspension systems instead of using single-input single-output sliding mode control as presented in all the previous work mentioned above. Although much research work has been devoted to the theoretical development, analysis and computer simulation of multivariable sliding mode control in the past decade, little experimental evaluation exist in the literature (Hung *et al.*, 1993).

While preparing this article, we found a similar study (Tian *et al.*, 1994) in which a two-input two-output sliding mode control was applied to a magnetic bearing system with experimental results. In the design method proposed by Tian *et al.* (1994), parameter variations are not taken into consideration, and the characteristics of the system dynamics can not be clearly defined in a physical sense. The effects of parameter variations and the physical meaning of system dynamics are two important issues in the design of multivariable sliding mode control and should be considered seriously in any applications.

In this paper, we will propose a design and implementation method of two-input two-output sliding mode

control for a two-dimensional magnetic suspension system, considering parameter variations and external disturbances. Using this design method, the characteristics of system dynamics can be clearly specified in a physical sense. Experimental results will also be included to verify the theoretical expectations. The organization of this paper is as follows. We will first specify a magnetic suspension system, which involves the plane motion of a free body, as our experimental system, and formulate a state-space representation for it in Sect. II. Then, based on the Lyapunov function approach, a two-input two-output sliding mode control design for the experimental system will be described in Sect. III. In Sect. IV, we will describe how the designed controller is implemented by a digital signal processor, and then present experimental results to verify the capabilities of the designed controller in Sect. V. Finally, conclusions will be given in the last section.

II. System Description and Modeling

The configuration of the experimental system in this study is shown in Fig. 1. It is a two-dimensional magnetic suspension system which represents the plane motion of a free body under the control of electromagnetic forces. Such a plane motion often exists in general magnetic suspension systems; one typical example is the horizontal or vertical plane motion of a rotor in a magnetic bearing system.

In Fig. 1, the moving bar is constrained to translate only in the x-direction (vertical direction) and to rotate only about the y-axis. Two fixed electromagnets located at the opposite ends above the moving bar generate the forces f_l and f_r to control the air gaps x_l and x_r between the electromagnets and the moving bar, by which the location and orientation of the moving bar can be specified. Let x_c represent the translational

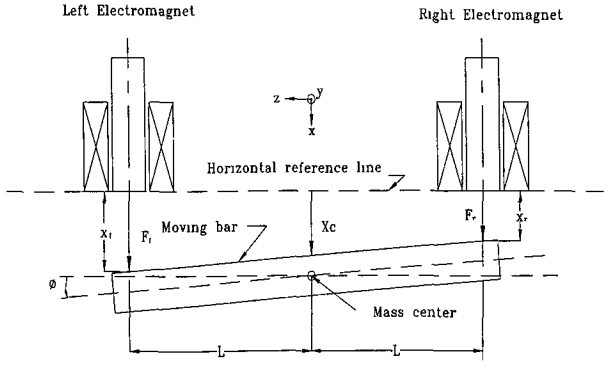

Fig. 1. Configuration of the experimental system.

displacement of the mass center of the moving bar from the reference line indicated in Fig. 1, and let ϕ be the rotational displacement of the moving bar from the reference line. Then, the equations of motion for the system are

$$M\ddot{x}_c = Mg - f_r - f_l \tag{1}$$

and $$J\ddot{\phi} = f_r L\cos\phi - f_l L\cos\phi, \tag{2}$$

in which M is the moving bar mass, g is the acceleration of gravity, J is the moment of inertia of the moving bar about the y-axis, and L is the distance from the mass center to the point on the moving bar at which the control force f_l or f_r is applied. It is assumed that the mass center of the moving bar coincides with its geometric center. For small perturbations, the following geometrical relations are valid (Youcef-Toumi and Reddy, 1992):

$$x_l = x_c + L\phi$$

$$x_r = x_c - L\phi$$

$$x_c = \frac{1}{2}(x_l + x_r). \tag{3}$$

Thus, Eq. (2) can be approximated by

$$\frac{J(\ddot{x}_l - \ddot{x}_r)}{2L^2} = f_r - f_l. \tag{4}$$

The control force f_l generated by the left electromagnet is modeled by the following equation (Hebbale, 1985):

$$f_l = \frac{\mu_0 A_l N_l^2 I_l^2}{2x_l^2}, \tag{5}$$

where μ_0 is the permeability of free space, A_l is the air gap area of one pole, N_l is the number of coil turns, and I_l is the coil current. Using the same notations in Eq. (5), the control force f_r generated by the right electromagnet is expressed by

$$f_r = \frac{\mu_0 A_r N_r^2 I_r^2}{2x_r^2}. \tag{6}$$

Substituting Eqs. (3), (5) and (6) into Eqs. (1) and (4), we obtain

$$\frac{M}{2}(\ddot{x}_l + \ddot{x}_r) = Mg - \frac{\alpha_l I_l^2}{x_l^2} - \frac{\alpha_r I_r^2}{x_r^2} \tag{7}$$

and $$\frac{J(\ddot{x}_l-\ddot{x}_r)}{2L^2}=\frac{\alpha_r I_r^2}{x_r^2}-\frac{\alpha_l I_l^2}{x_l^2}, \quad (8)$$

where $\alpha_l=\mu_0 A_l N_l^2/2$ and $\alpha_r=\mu_0 A_r N_r^2/2$. The corresponding state equations are

$$\dot{x}_{1l}=x_{2l}$$

$$\dot{x}_{2l}=g-(1+\frac{ML^2}{J})[\frac{\alpha I_l^2}{Mx_{12}^2}]$$

$$-(1-\frac{ML^2}{J})\frac{\alpha I_r^2}{Mx_{1r}^2}]$$

$$\dot{x}_{1r}=x_{2r}$$

$$\dot{x}_{2r}=g-(1-\frac{ML^2}{J})[\frac{\alpha I_l^2}{Mx_{12}^2}]$$

$$-(1+\frac{ML^2}{J})\frac{\alpha I_r^2}{Mx_{1r}^2}], \quad (9)$$

where $x_{1l}=x_l$, $x_{1r}=x_r$, and $\alpha=\alpha_l=\alpha_r$.

At an equilibrium position $x_{1l}=x_{1r}=x_0$, let the corresponding coil current be $I_l=I_r=I_0$. Thus, around the equilibrium point (x_0, I_0),

$$x_{1l}=x_0+e_{1l}$$

$$x_{1r}=x_0+e_{1r}$$

$$I_l=I_0+i_l$$

$$I_r=I_0+i_r, \quad (10)$$

where e_{1l}, e_{1r}, i_l and i_r are the small perturbations of the quantities x_{1l}, x_{1r}, I_l and I_r, respectively. Linearizing the state equations of Eq. (9) about the equilibrium point (x_0, I_0) gives the following linear state equations in matrix form:

$$\dot{E}=AE-Bu, \quad (11)$$

where $E=[e_{1l}\ e_{2l}\ e_{1r}\ e_{2r}]^T$, $u=[i_l\ i_r]^T$,

$$A=\begin{bmatrix}0 & 1 & 0 & 0\\ a_{21} & 0 & a_{23} & 0\\ 0 & 0 & 0 & 1\\ a_{41} & 0 & a_{43} & 0\end{bmatrix},$$

in which $a_{21}=a_{43}=(1+\frac{ML^2}{J})(\frac{g}{I_0})\sqrt{\frac{Mg}{2\alpha}}$ and

$$a_{23}=a_{41}=(1-\frac{ML^2}{J})(\frac{g}{I_0})\sqrt{\frac{Mg}{2\alpha}},$$

and $B=\begin{bmatrix}0 & 0\\ b_{21} & b_{22}\\ 0 & 0\\ b_{41} & b_{42}\end{bmatrix}$, in which $b_{21}=b_{42}=(1+\frac{ML^2}{J})(\frac{g}{I_0})$

and $b_{22}=b_{41}=(1-\frac{ML^2}{J})(\frac{g}{I_0})$.

When considering external force disturbances, Eq. (11) is modified as

$$\dot{E}=AE-Bu+D, \quad (12)$$

where $D=[0\ d_l\ 0\ d_r]^T$, in which d_l and d_r represent external disturbing forces.

The experimental system based on the configuration of Fig. 1 has been built; its mechanical structure is shown in Fig. 2. We have also made an optoelectronic position sensor to measure the air gaps x_l and x_r, the circuit diagram of which is shown in Fig. 3, in which the optoelectronic device PL2826 is from Hamamats Co. in Japan. The sensitivity of the sensor is 1.8V/mm, and the noise level is about 4mV peak-to-peak. Two U-shaped electromagnets fixed at opposite ends above the moving bar are identical and are driven by a current-source power amplifier whose maximum current is 2.5 amperes. The moving bar is made of an aluminium bar with a piece of ferromagnetic material mounted at each end. The mass of the moving bar is M_1=1.86 kg, and its moment of inertia is J_1=0.02445 kg-m^2. Both the mass and the moment of inertia can be changed by placing an additional weight

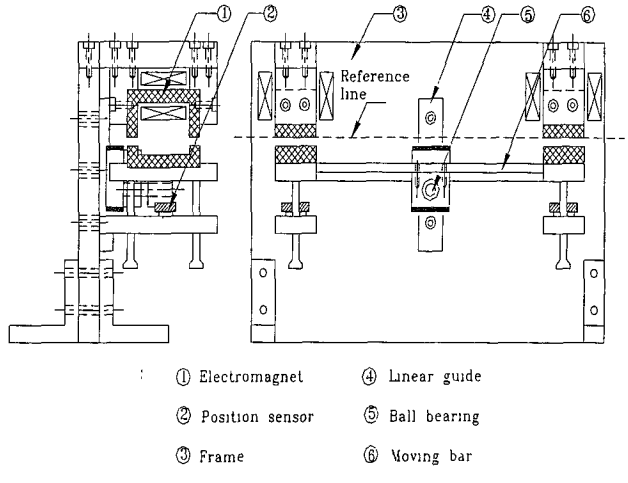

Fig. 2. Mechanical structure of the experimental system.

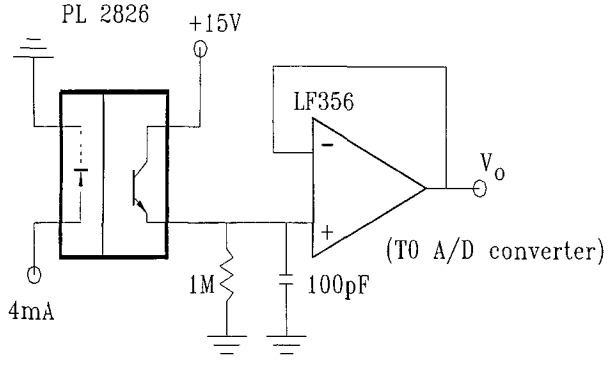

Fig. 3. Circuit diagram of the optoelectronic sensor.

Table 1. Parameters of the Experimental System

Area of one magnetic pole (A)	0.0004	m^2
Number of coil turns (N)	700	
Dimension of moving bar (L)	0.135	m
Mass of moving bar (kg)	M_1=1.86	kg
	M_2=2.767	kg
Moment of inertia of moving bar (J)	J_1=0.02445	kg-m^2
	J_2=0.02667	kg-m^2

of 0.907 kg on the moving bar, resulting in M_2=2.767 kg and J_2=0.02667 kg-m^2. The parameters of the experimental system are summarized in Table 1.

III. Sliding Mode Controller Design

As usual, the design procedure consists of two major phases: the first phase is construction of a set of switching functions so that the desired sliding dynamics can be obtained; the second phase is finding a control law such that the so-called sliding mode condition can be satisfied.

In constructing a set of switching functions, we first treat the system of Eq. (12) as single-input subsystems; namely, a right subsystem and left subsystem. The right subsystem is associated with the input i_r and the output e_{1r}; the left subsystem, the input i_l and the output e_{1l}. Then, we define the switching functions as

$s_r=c_1e_{1r}+e_{2r}$ for the right subsystem

and $s_l=c_1e_{1l}+e_{2l}$ for the left subsystem, where $c_1>0$. The same sliding mode dynamics are expected for both subsystems because the same parameter c_1 is used in both switching functions. Consequently, the dynamic characteristics of the whole system can be clearly defined by a single characteristic equation as

$$c_1\dot{e}(t)+e(t)=0, \tag{13}$$

where $e(t)$ represents a position error at any point on the moving bar. The switching functions defined above can be represented in matrix form as

$$S=CE, \tag{14}$$

where $S=\begin{bmatrix} s_l \\ s_r \end{bmatrix}$, $C=\begin{bmatrix} c_1 & 1 & 0 & 0 \\ 0 & 0 & c_1 & 1 \end{bmatrix}$ and $E=[e_{1l}\ e_{2l}\ e_{1r}\ e_{2r}]^T$.

The controller design is based on the Lyapunov function approach. For a multivariable sliding mode control system, a useful Lyapunov function has proven to be difficult to find (Utkin, 1978; DeCarlo *et al.*, 1988). Fortunately, we have found that the system in this study possesses a special property, that is, the matrix $(CB)^{-1}$, where B is the gain matrix of the system of Eq. (11) and is a positive-definite symmetric matrix. Based on this finding, we obtain a useful Lyapunov function candidate. The following is given to prove that the matrix $(CB)^{-1}$ is a positive-definite symmetric matrix:

$$CB=\begin{bmatrix} c_1 & 1 & 0 & 0 \\ 0 & 0 & c_1 & 1 \end{bmatrix}\begin{bmatrix} 0 & 0 \\ b_{21} & b_{22} \\ 0 & 0 \\ b_{41} & b_{42} \end{bmatrix}=\begin{bmatrix} b_{21} & b_{22} \\ b_{41} & b_{42} \end{bmatrix}$$

$$(CB)^{-1}=\begin{bmatrix} b_{21} & b_{22} \\ b_{41} & b_{42} \end{bmatrix}^{-1}=\begin{bmatrix} \overline{b}_{11} & \overline{b}_{12} \\ \overline{b}_{21} & \overline{b}_{22} \end{bmatrix},$$

where $\overline{b}_{11}=\overline{b}_{22}=(\frac{I_0}{4g})(1+\frac{J}{ML^2})$; $\overline{b}_{12}=\overline{b}_{21}=(\frac{I_0}{4g})$ $\cdot(1-\frac{J}{ML^2})$.

The determinant of $(CB)^{-1}$ is

$$\left|(CB)^{-1}\right|=(\frac{I_0}{2g})^2\frac{J}{ML^2}>0.$$

In addition, $\overline{b}_{11}>0$. By the Sylvester criterion (Chen, 1984), $(CB)^{-1}$ is a positive-definite symmetric matrix.

A Lyapunov function candidate is defined as

$$V(S)=\frac{1}{2}S^TRS, \tag{15}$$

where R is a positive-definite symmetric 2×2 matrix. If

$$\dot{V}(S)<0, \tag{16}$$

then S approaches zero asymptotically, and the sliding condition is satisfied (Utkin, 1978). From Eqs. (12) and (14), the time derivative of $V(S)$ becomes

$$\dot{V}(S)=S^T R\dot{S}=S^T R[(CA)E-(CB)u+D]. \quad (17)$$

Let $R=(CB)^{-1}$; then Eq. (17) becomes

$$\dot{V}(S)=S^T[(CB)^{-1}(CA)E]-S^T u+S^T(CB)^{-1}D. \quad (18)$$

The term $S^T u=s_r i_r+s_l i_l$ in Eq. (18) shows that the control inputs i_l and i_r are decoupled with respect to the switching functions s_l and s_r, so that the existence of a proper control law to satisfy the sliding condition $\dot{V}(S)<0$ is ensured. The control law is designed as

$$i_l=(k_{pl}e_{1l}+k_{dl}e_{2l})+K_l E+k_{zl}z_l+\eta_l \text{sign}(s_l), \quad (19)$$

in which k_{pl} and k_{dl} are constant gains, $K_l=[k_{1l}\ k_{2l}\ k_{3l}\ k_{4l}]$ is the switching gain matrix, $z_l=\int_0^t e_{1l}\,dt$, $\text{sign}(s_l)=\begin{cases}+1 & \text{if } s_l>0\\ -1 & \text{if } s_l<0\end{cases}$, k_{zl}, η_l are both switching gains, and

$$i_r=(k_{pr}e_{1r}+k_{dr}e_{2r})+K_r E+k_{zr}z_r+\eta_r \text{sign}(s_r). \quad (20)$$

The meaning of the symbols in Eq. (20) is exactly the same as in Eq. (19). Substituting Eqs. (19) and (20) into Eq. (18), we obtain

$$\begin{aligned}\dot{V}(S)=&[(a_{21}\overline{b}_{11}+a_{41}\overline{b}_{12}-k_{pl})-k_{1l}]e_{1l}s_l\\ &+[(\overline{b}_{11}c_1-k_{dl})-k_{2l}]e_{2l}s_l\\ &+[(a_{23}\overline{b}_{11}+a_{43}\overline{b}_{12})-k_{3l}]e_{1r}s_l\\ &+(\overline{b}_{12}c_1-k_{4l})e_{2r}s_l-k_{5l}z_l s_l\\ &+[(\overline{b}_{11}d_l+\overline{b}_{12}d_r)-\eta_l \text{sign}(s_l)]s_l\\ &+[(a_{21}\overline{b}_{21}+a_{41}\overline{b}_{22})-k_{1r}]]e_{1l}s_r\\ &+(\overline{b}_{21}c_1-k_{2r})e_{2l}s_r\\ &+[(a_{23}\overline{b}_{21}+a_{43}\overline{b}_{22}-k_{pr})-k_{3r}]e_{1r}s_r\\ &+[(\overline{b}_{22}c_1-k_{dr})-k_{4r}]e_{2r}s_r-k_{5r}z_r s_r\\ &+[(\overline{b}_{21}d_l+\overline{b}_{22}d_r)-\eta_r \text{sign}(s_r)]s_r. \end{aligned} \quad (21)$$

In order to satisfy $\dot{V}(S)<0$, the control gains are chosen as

$$k_{1l}=\begin{cases}k_{1l}^+>\max(a_{21}\overline{b}_{11}+a_{41}\overline{b}_{12}-k_{pl})\\ \quad \text{when } e_{1l}s_l>0\\ k_{1l}^-<\min(a_{21}\overline{b}_{11}+a_{41}\overline{b}_{12}-k_{pl})\\ \quad \text{when } e_{1l}s_l<0\end{cases}$$

$$k_{2l}=\begin{cases}k_{2l}^+>\max(\overline{b}_{11}c_1-k_{dl}) & \text{when } e_{2l}s_l>0\\ k_{2l}^-<\min(\overline{b}_{11}c_1-k_{dl}) & \text{when } e_{2l}s_l<0\end{cases}$$

$$k_{3l}=\begin{cases}k_{3l}^+>\max(a_{23}\overline{b}_{11}+a_{43}\overline{b}_{12}) & \text{when } e_{1r}s_l>0\\ k_{3l}^-<\min(a_{23}\overline{b}_{11}+a_{43}\overline{b}_{12}) & \text{when } e_{1r}s_l<0\end{cases}$$

$$k_{4l}=\begin{cases}k_{4l}^+>\max(\overline{b}_{12}c_1) & \text{when } e_{2r}s_l>0\\ k_{4l}^-<\min(\overline{b}_{12}c_1) & \text{when } e_{2r}s_l<0\end{cases}$$

$$k_{5l}=\begin{cases}k_{5l}^+>0 & \text{when } z_l s_l>0\\ k_{5l}^-<0 & \text{when } z_l s_l<0\end{cases}$$

$$\eta_1>\max(\overline{b}_{11}d_l+\overline{b}_{12}d_r)\quad \forall s_l$$

$$k_{1r}=\begin{cases}k_{1r}^+>\max(a_{21}\overline{b}_{21}+a_{41}\overline{b}_{22}) & \text{when } e_{1l}s_r>0\\ k_{1r}^-<\min(a_{21}\overline{b}_{21}+a_{41}\overline{b}_{22}) & \text{when } e_{1l}s_r<0\end{cases}$$

$$k_{2r}=\begin{cases}k_{2r}^+>\max(\overline{b}_{21}c_1) & \text{when } e_{2l}s_r>0\\ k_{2r}^-<\min(\overline{b}_{21}c_1) & \text{when } e_{2l}s_r<0\end{cases}$$

$$k_{3r}=\begin{cases}k_{3r}^+>\max(a_{23}\overline{b}_{21}+a_{43}\overline{b}_{22}-k_{pr})\\ \quad \text{when } e_{1r}s_r>0\\ k_{3r}^-<\min(a_{23}\overline{b}_{21}+a_{43}\overline{b}_{22}-k_{pr})\\ \quad \text{when } e_{1r}s_r<0\end{cases}$$

$$k_{4r}=\begin{cases}k_{4r}^+>\max(\overline{b}_{22}c_1-k_{dr}) & \text{when } e_{2r}s_r>0\\ k_{4r}^-<\min(\overline{b}_{22}c_1-k_{dr}) & \text{when } e_{2r}s_r<0\end{cases}$$

$$k_{5r}=\begin{cases}k_{5r}^+>0 & \text{when } z_r s_r>0\\ k_{5r}^-<0 & \text{when } z_r s_r<0\end{cases}$$

$$\eta_r>\max(\overline{b}_{21}d_l+\overline{b}_{22}d_r)\quad \forall s_r \quad (22)$$

Several remarks are made below about the above design method:

(1) The control law of Eq. (19) can be divided into two parts: one part which comprises $k_{pl}e_{1l}$ and $k_{pd}e_{2l}$ is called the continuous part because k_{pl} and k_{dl} are constant gains which must be specified before the switching gains are determined; the other part which comprises the remaining terms with switching gains is called the switching part because all the gains in this part are switching gains. The continuous part shall be implemented by an analog circuit to help stabilize the magnetic suspension system in a continuous-time base while the switching part

shall be implemented by a microcomputer because this part needs a considerable amount of algebraic computation and logic decision. When a sliding mode controller is implemented by a microcomputer, the chattering problem, which is associated with oscillation of output response mainly due to switching control actions, becomes more severe because of sampling effects. From our long-time observations, we have found that the chattering problem can be significantly improved by introducing this continuous part in the control law. The same statements can be made for the control law of Eq. (20).

(2) In the control law, the switching term k_lE or k_rE can take care of the variations of the system parameters. On the other hand, the integral term $k_{zl}\int_0^t e_{1l}\,dt$ or $k_{zr}\int_0^t e_{1r}\,dt$ is used to accomodate a step-type disturbance and to reduce the steady-state error while the term $\eta_l\text{sign}(s_l)$ or $\eta_r\text{sign}(s_r)$ is given for other types of disturbances if needed.

(3) The decoupling of control inputs with respect to switching functions is usually accomplished by the so-called diagonalization method proposed by Utkin (1978). The diagonalization method involves a non-singular transformation of switching functions such as $S^*=Q(CB)^{-1}S$, where S is the original switching function vector, and Q is a constant diagonal matrix. When the matrix B has uncertainties, using the transformed switching function vector S^* in implementation is impractical. Thus, the diagonalization method is not applicable to this study.

IV. Controller Implementation

The equilibrium position x_0=1mm and the corresponding coil current I_0=0.436 amp were used in this study. In the control laws of Eqs. (19) and (20), $k_{pl}=k_{pr}$=657.5, $k_{dl}=k_{dr}$=0.75 were chosen for the continuous parts. The value of each element in the switching gain matrix K_l or K_r can then be determined by Eq. (22), once the value of the parameter c_1 in the switching functions s_l and s_r is decided. Two values of the parameter c_1 (c_1=10 and 40) were used in the experiments in order to demonstrate that the system dynamics were really controlled by the sliding mode dynamics of Eq. (13). As for the integral gain k_{zl} or k_{zr}, its value was tuned on-line because there is no theoretical constraint on this value as shown in Eq. (22). Due to the lack of adequate hardware in the experimental system, experiments concerning external force disturbances other than a step-type disturbance could not be conducted; therefore, the term $\eta_l\text{sign}(s_l)$ or $\eta_r\text{sign}(s_r)$ for disturbance rejection was omitted in the controller implementation.

The continuous part of the control was implemented by analog circuits of a few operational amplifiers while the switching part was implemented by a single TMS320C25 digital signal processor. The control program in TMS320C25 assembly language was written to compute the control law and was stored in the TMS320C25 system board which resided in a personal computer. The execution time of the control program was less than 1 ms; thus 1 ms was taken as the sampling period.

In executing the control program, both position and velocity information about the moving bar was needed. The position signals were provided by the optoelectronic position sensors, and the velocity signals were obtained from the rate of change of the position signals, using an analog circuit or digital computation.

V. Experimental Results

The experimental objective was to stabilize the moving bar horizontally at a distance of 1mm below the reference line, that is, x_l(left air gap)=x_r(right air gap)=1 mm. Meanwhile, it was expected that the response x_l or x_r should be governed by the sliding mode equation $c_1\dot{e}(t)+e(t)=0$ in Eq. (13). Because the sliding mode equation was a first-order differential equation with the adjustable parameter c_1, no overshooting was expected.

Figure 4 shows the position response of the moving bar from an initial position, when the parameter c_1=40 is used for the sliding mode equation. Such a step response is described by the measured responses of x_l and x_r from the initial value of 1.45 mm to the desired

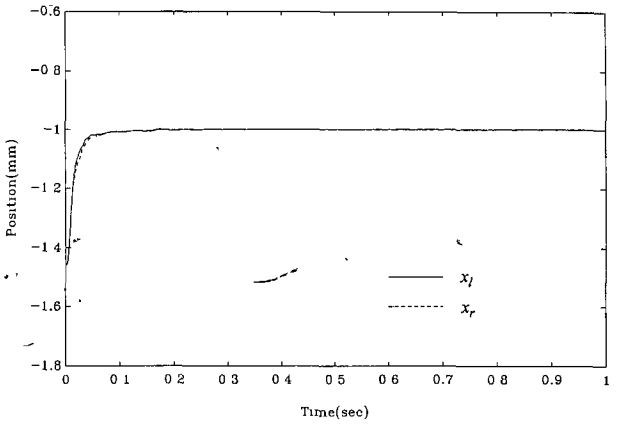

Fig. 4. Step response of the moving bar described by air gap responses of x_l and x_r.

value of 1 mm. Two response curves in Fig. 4 are nearly identical and both exhibit no significant overshooting. So, this experimental result agrees well with the theoretical expectation because the responses of x_l and x_r were under the control of the same first-order sliding mode equation. The steady-state error responses associated with the response curves of x_l and x_r in Fig. 4 are shown in Fig. 5. A test similar to the previous one was conducted, but with two different values of the parameter c_1 for the sliding mode equation. The test results are shown in Fig. 6. For the response of x_l in Fig. 6, two curves with a significant difference in speed of response are associated with two different values of c_1. This further demonstrates that the system response was effectively controlled by the predetermined sliding mode equation, which was specified by the value of c_1. In order to test the controller robustness against the simultaneous presence of parameter variations and a step-type external disturbance, a weight of 0.907 kg was suddenly dropped on the moving bar which was being stabilized at the desired position. The results of this test are shown in Fig. 7. Two response curves are nearly identical and fulfill the theoretical expectations again. In all the tests, the steady-state position error was kept within 0.005 mm, which nearly reached the resolution limit of the optoelectronic sensor used in the experimental system.

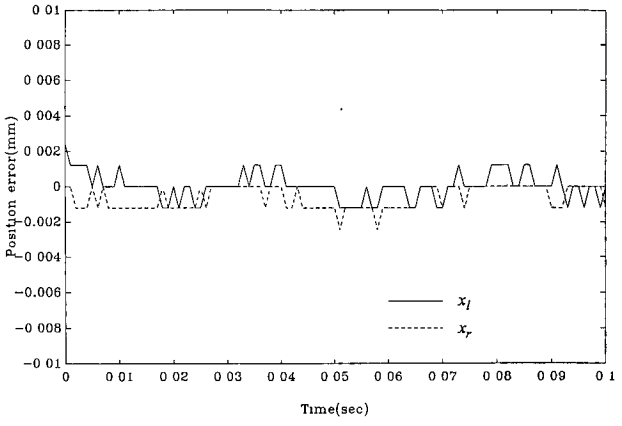

Fig. 5. Steady-state error response of x_l and x_r.

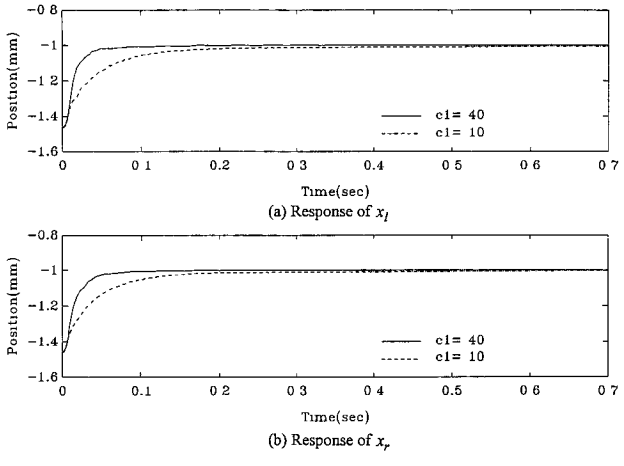

Fig. 6. Step responses of the moving bar with different sliding mode dynamics.

VI. Conclusion

A controller based on the proposed two-input two-output sliding mode control design method for an experimental magnetic suspension system was successfully implemented by a single unit digital signal processor and a simple analog circuit. The experimental results verified that the experimental system subject to significant parameter variations and an external disturbance could be reliably controlled by the predetermined sliding mode dynamics, which were clearly defined in a physical sense. We also found that the chattering phenomenon inherent in sliding mode control could be greatly improved by introducing a continuous-time state feedback control implemented by an analog circuit. Thus, a steady-state position error of within 0.005 mm was achieved in all the experiments. Such accuracy was limited by the optoelectronic position sensor made for this study.

This paper has presented a practical design and implementation method of multivariable sliding mode control for a two-degree-of-freedom magnetic suspension system. A controller design for general magnetic suspension systems with a greater degree of freedom could be based on the the proposed method instead of using single-input single-output sliding mode control

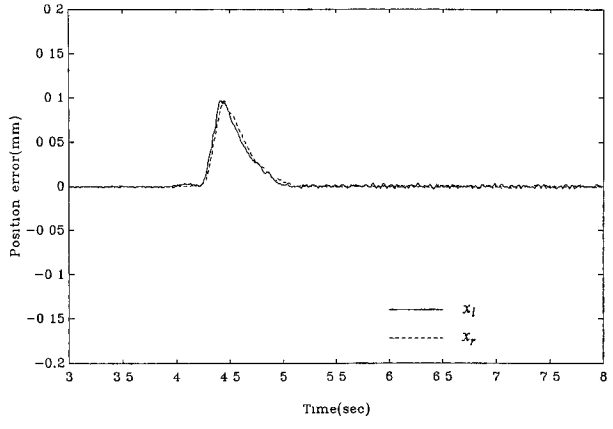

Fig. 7. Response of robustness test against parameter variations and step-type external disturbance.

techniques. Furthermore, this paper has also provided a real case of experimental study on multivariable sliding mode control.

Acknowledgment

This work was supported by the National Science Council under Contract No. NSC 83-0422-E007-052.

References

Chen, C. T. (1984) *Linear System Theory and Design*. Harcourt Brace Jovanovich College Publishers, U.S.A.

Cho, D., Y. Kato, and D. Spilman (1993) Sliding mode and classical controllers in magnetic levitation systems. *IEEE Control Systems*, 42-48.

Cui, W. M. and K. Nonami (July, 1992) H^∞ control of flexible rotor-magnetic bearing systems. Proceedings of the Third International Symposium on Magnetic Bearings, Alexandria, VA, U.S.A., 505-514.

DeCarlo, R., S. Zak, and G. Matthews (1988) Variable structure control of nonlinear multivariable systems. *Proceedings of the IEEE*, **3**, 212-232.

Hebbale, K. (1985) A theoretical model for the study of nonlinear dynamics of magnetic bearings. Ph.D. Dissertation, Cornell University, U.S.A.

Hung, J. Y., W. Gao, and J. C. Hung (1993) Variable structure control: A survey. *IEEE Trans. on Industrial Electronics*, **1**, 2-21.

Hwang, G., W. Hwang, and S. Lin (1992) A Robust control for magnetic suspension systems. *Journal of CSME*, **3**, 258-264.

Hwang, G. C. (1992) A study of robust control for magnetic suspension systems. Ph.D. Dissertation. National Tsing-Hua University, Hsin-Chu, Taiwan, R.O.C.

Jayawant, B. V. (1988) Electromagnetic suspension and levitation techniques. *Proceedings Royal Society, London, Part A*, **416**, 245-320 (editor).

Matsumura, F. (1993) *Magnetic Suspension Technology*. Corona Publishing Co., Japan (in Japanese).

Matsumura, F., F. Fujita, and M. Shimizu (1991) Robust stabilization of a magnetic suspension system using H^∞ control theory. *Electrical Engineering in Japan*, **111**, 117-124.

Misovec, K., F. Flynn, and B. Johnson (Sept., 1990) Sliding mode control of magnetic suspensions for precision pointing and tracking applications. Workshop on Aerospace Applications of Magnetic Suspension Technology, Hampton, VA, U.S.A., 144-163.

Nonami, K. and H. Yamaguchi (July, 1992) Robust control of magnetic bearings by means of sliding mode control. *J. of Japanese Society of Mech. Engineering, Part C*, **545**, 106-111.

Oguchi, K. and K. Okada (1992) Contactless starting and positioning of a steel ball in single-axis magnetic suspension device by variable structure control. Proceedings of the Third International Symposium on Magnetic Bearings, Alexandria, VA, U.S.A., 60-69.

Tian, H., K. Nonami, and M. Kubota (1994) Discrete time sliding mode control of flexible rotor magnetic bearing system with variable structure system observer. *J. of Japanese Society of Mech. Engineering, Part C*, **569**, 94-101.

Utkin, V. (1978) *Sliding Modes and Their Application in Variable Structure Systems*. MIR publisher, Moscow, Russia.

Youcef-Toumi, K. and S. Reddy (1992) Dynamic analysis and control of high speed and high precision active magnetic bearings. *Trans. of the ASME, J. of Dynamic Systems, Measurement, and Control*, **114**, 623-633.

磁浮系統之多變數滑動模式控制

洪聯馨　林世昌

清華大學動力機械研究所

摘　要

本文針對磁浮系統，考慮其參數變動及外界干擾，提出一種實用的多變數滑動模式控制設計方式及實施方法。根據Lyapunov函數方法，本文所提出的設計方法可保證獲得滿足滑動模式存在條件的控制律。所設計的控制器成功地實施於磁浮實驗系統。實驗結果顯示實驗系統確實受控於預設之滑動模式動態，並且驗證控制器的性能。此外，本文亦提供一個多變數滑動模式控制實驗研究的實例。